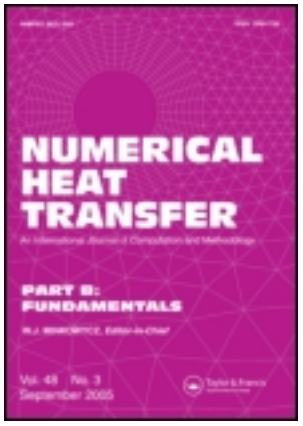

Numerical Heat Transfer, Part B: Fundamentals: An International Journal of Computation and Methodology

Publication details, including instructions for authors and subscription information:
http://www.tandfonline.com/loi/unhb20

An Improved Numerical Scheme for the SIMPLER Method on NonOrthogonal Curvilinear Coordinates: SIMPLERM

Z. G. Qu [a], W. Q. Tao [a] & Y. L. He [a]

[a] State Key Laboratory of Multiphase Flow in Power Engineering, School of Energy & Power Engineering, Xi'an Jiaotong University, Xi'an, Shaanxi, People's Republic of China

Available online: 24 Feb 2007

To cite this article: Z. G. Qu, W. Q. Tao & Y. L. He (2007): An Improved Numerical Scheme for the SIMPLER Method on NonOrthogonal Curvilinear Coordinates: SIMPLERM, Numerical Heat Transfer, Part B: Fundamentals: An International Journal of Computation and Methodology, 51:1, 43-66

To link to this article: http://dx.doi.org/10.1080/10407790600682797

Numerical Heat Transfer, Part B, 51: 43–66, 2007

ISSN: 1040-7790 print/1521-0626 online
DOI: 10.1080/10407790600682797

Taylor & Francis
Taylor & Francis Group

AN IMPROVED NUMERICAL SCHEME FOR THE SIMPLER METHOD ON NONORTHOGONAL CURVILINEAR COORDINATES: SIMPLERM

Z. G. Qu, W. Q. Tao, and Y. L. He

State Key Laboratory of Multiphase Flow in Power Engineering, School of Energy & Power Engineering, Xi'an Jiaotong University, Xi'an, Shaanxi, People's Republic of China

In this article, an improved numerical algorithm named SIMPLERM is proposed for incompressible fluid flow computations on the nonstaggered and nonorthogonal curvilinear grid system. In the proposed algorithm, the contravariant velocities are chosen as the cell face velocities and the Cartesian components as the primary variables. The velocity underrelaxation factor is incorporated into the momentum interpolation, and special treatment is adopted to avoid the underrelaxation factor dependence of the velocity solution. In addition, a $1-\delta$ pressure difference is introduced into the interfacial contravariant velocity determination. Compared with the existing implementation methods of the SIMPLE family on nonstaggered and nonorthogonal grids, the SIMPLERM algorithm can guarantee the coupling between velocity and pressure, underrelaxation independence of the solution, and satisfaction of the conservation law, while still possessing sufficient robustness.

INTRODUCTION

For numerical prediction of fluid flow and heat transfer in complex geometries, numerical methods of nonorthogonal, body-fitted coordinates may be adopted in which governing equations are converted from the physical domain to the computational domain. The grid arrangements, choice of dependent variable of momentum equations, and pressure–velocity coupling are three key issues for the solution of incompressible flow problems.

The coupling between velocity and pressure can be naturally guaranteed in the staggered grid arrangement, but this arrangement is inconvenient for code development in a curvilinear body-fitted grid or an unstructured grid, especially for 3-D computation. This complexity can be greatly alleviated by using a nonstaggered grid system. However, use of a nonstaggered grid may lead to other undesirable features of numerical solutions.

For a nonstaggered grid the key issue is how to eliminate the decoupling between pressure and velocity. In the 1980s, the momentum interpolation method

Received 15 December 2005; accepted 15 February 2006.

The work reported here is supported by the National Natural Science Foundation of China (50476046, 50425620, 50576069) and the Basic Research Program of China (2006CB601203).

Address correspondence to Wen-Quen Tao, School of Energy & Power Engineering, Xi'an Jiaotong University, Xi'an, Shaanxi 710049, People's Republic of China. E-mail: wqtao@mail.xjtu.edu.cn

NOMENCLATURE

A	surface area	U_{lid}	moving velocity of lid
A_P, A_E, A_W, A_N, A_S	coefficients in the discretized equation	x_ξ, x_η, y_ξ, y_η	geometry factor
		x, y	coordinates in physical domain
b	source term		
B	coefficient in pressure or pressure-correction equation	X, Y	coordinates in computational domain
		α	underrelaxation factor
C	coefficient in pressure or pressure-correction equation	Γ	nominal diffusion coefficient
		$\delta\xi$, $\delta\eta$	distance between two adjacent grid points in ζ and η directions
E	time-step multiple		
f	interpolation factor		
F	flow rate	$\Delta\xi$, $\Delta\eta$	distance between two adjacent interfaces in ζ and η directions
flow_{ch}	characteristic (reference) flow rate		
J	Jacobi factor	ζ	coordinate in computational domain
L	length, m		
p	pressure	η	coordinate in computational domain
p'	pressure correction		
$\bar{p}_\eta$	average value of pressure gradient in η direction	μ	fluid dynamic viscosity
		ρ	fluid density
		ϕ	general variable
$\bar{p}_\xi$	average value of pressure gradient in ξ direction	**Subscripts**	
		e, w, n, s	cell surface
Pr	Prandtl number	max	maximum
Re	Reynolds number	P, E, N, S, W	grid point
RS_{max}	relative mass flow rate unbalance of control volume	nb	neighboring points
		non	nonorthogonal term
		u, v	referring to u, v momentum equation
u, v	velocity component in x, y directions		
u', v'	velocity correction	**Superscripts**	
$\hat{u}$, $\hat{v}$	pseudo-velocity	i	intermediate value of Cartesian coordinates in iteration
U, V	contravariant velocity		
$\hat{U}$, $\hat{V}$	contravariant pseudo-velocity	0	previous iteration
$\overline{U}$, $\overline{V}$	contravariant velocity obtained by linear interpolation	$*$	intermediate value in iteration
		$\rightarrow$	vector
U', V'	contravariant velocity correction	$'$	correction
		—	mean value

(MIM) on the nonstaggered grid was first proposed by Rhie and Chow [1] to overcome the decoupling difficulty. It was subsequently refined by Peric [2] and Majumdar [3]. Later, Majumdar [4] and Miller and Schmidt [5] found that the Rhie and Chow method leads to dependence of the solution on an underrelaxation factor to some extent, despite damping out the checkerboard pressure distribution. To remedy this undesirable situation, Majumdar [4] provided the modified momentum interpolation method (MMIM), which was later adapted by Choi [6] for unsteady

flow. An easy technique introduced by Kobayashi and Pereira [7] is to set the underrelaxation factor to $\alpha = 1$ before momentum interpolation, but this may lead to deterioration of the robustness of the algorithm to at least some extent.

Based on a number of previous studies on the nonstaggered (or collocated) grid system, the present authors put forward four fundamental requirements for developing a good numerical algorithm in the nonstaggered grid system [8]. The four requirements are that: (1) the algorithm can avoid the checkerboard pressure distribution; (2) the converged solution is independent of the underrelaxation factor; (3) the algorithm possesses required robustness; and (4) the conservation laws, both physical and geometric, should be satisfied as much as possible.

On a nonorthogonal collocated grid, the first problem encountered in the development of a numerical algorithm is the choice of dependent variables, and different choice lead to different solution algorithms for pressure and velocity coupling. Shyy and Vu [9] indicated that it is an appropriate choice to use Cartesian velocity components as the primary variables and contravariant velocity components as cell face velocities to satisfy the conservation law (both physical and geometric) in the discrete form.

For curvilinear nonorthogonal coordinates, the implementation of SIMPLE, SIMPLER, and the modified algorithm SIMPLEM have been proposed in [10]. When in introducing these three algorithms for curvilinear nonorthogonal coordinates, Acharya and Moukalled [10] did not pay special attention to the underrelaxation factor issue. Kobayashi and Pereira [7, 11] proposed the SIMPLES algorithm, which could eliminate the effect of underrelaxation factor but reduced the robustness to some extent. On the other hand, in the SIMPLE method proposed in [10], an additional pressure gradient correction term was added to the cell-face contravariant velocity to guarantee the coupling between velocity and pressure. However, this additional term can demolish the local mass conservation.

Choi et al. [12] proposed a calculation procedure for the SIMPLE algorithm to eliminate the effect of the underrelaxation factor and avoid the additional correction term. It was found that if the contravariant velocity was selected as cell face velocity, an unstable convergence history might occur when the grid nonorthogonality was significant, so the covariant velocity components were chosen as the cell face velocities. However, using the covariant velocity components as cell face velocities will not fully guarantee the geometric conservation law in the discrete form, as indicated in [9].

From the above brief review, it can be seen that in the current literature there is no algorithm for nonstaggered grids which can simultaneously satisfy the above four requirements. The major purpose of this study is to propose a new algorithm, SIMPLERM, which can simultaneously satisfy the four requirements to a great degree for the solution of flow fields in nonorthogonal collocated grids.

GOVERNING EQUATIONS AND DISCRETIZATION

For convective-diffusion problems in two-dimensional Cartesian coordinates, the governing equations can be expressed as

$$\frac{\partial(\rho u\phi)}{\partial x}+\frac{\partial(\rho v\phi)}{\partial y}=\frac{\partial}{\partial x}\left(\Gamma\frac{\partial\phi}{\partial x}\right)+\frac{\partial}{\partial y}\left(\Gamma\frac{\partial\phi}{\partial y}\right)+R(x,y) \tag{1}$$

Table 1. Correspondence among ϕ, Γ_ϕ, and R_ϕ

ϕ	Γ_ϕ	R_ϕ
u	η	$-\frac{\partial p}{\partial x}$
v	η	$-\frac{\partial p}{\partial y}$
T	$\frac{\mu}{\mathrm{Pr}}$	0

where ϕ is the general variable and R is the source term shown in Table 1. In collocated nonorthogonal curvilinear coordinates, the curvilinear coordinates are introduced in the following way:

$$x = x(\xi, \eta) \tag{2}$$

$$y = y(\xi, \eta) \tag{3}$$

The governing equations are converted to the computational domain, and the transferred equation can be expressed as

$$\frac{1}{J}\frac{\partial(\rho U\phi)}{\partial\xi} + \frac{1}{J}\frac{\partial(\rho V\phi)}{\partial\eta} = \frac{1}{J}\frac{\partial}{\partial\xi}\left[\frac{\Gamma}{J}(\alpha\phi_\xi - \beta\phi_\eta)\right] + \frac{1}{J}\frac{\partial}{\partial\eta}\left[\frac{\Gamma}{J}(-\beta\phi_\xi + \gamma\phi_\eta)\right] + S(\xi, \eta) \tag{4}$$

In Eq. (4), α, β, γ, and J are geometry factors and U, V are contravariant velocity components. The above parameters are defined as follows:

$$\alpha = x_\eta^2 + y_\eta^2 \qquad \beta = x_\xi x_\eta + y_\xi y_\eta \qquad \gamma = x_\xi^2 + y_\xi^2 \tag{5}$$

$$J = x_\xi y_\eta - x_\eta y_\xi \tag{6}$$

$$U = uy_\eta - vx_\eta \tag{7}$$

$$V = vy_\xi - vx_\xi \tag{8}$$

The source terms for the converted u and v equations include the transferred pressure gradients, which can be expressed as

$$\frac{\partial p}{\partial x} = \frac{1}{J}(y_\eta\phi_\xi - y_\eta\phi_\eta) \tag{9}$$

$$\frac{\partial p}{\partial y} = \frac{1}{J}(-x_\eta\phi_\xi - x_\xi\phi_\eta) \tag{10}$$

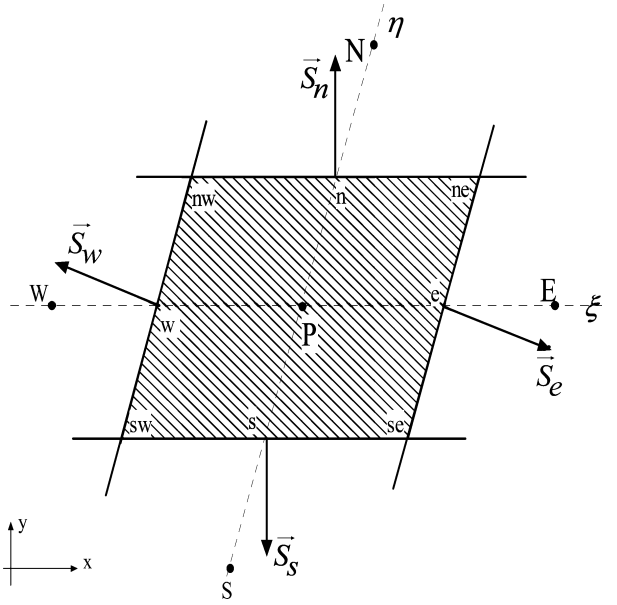

Figure 1. Control volume in curvilinear coordinates.

The control volumes in the physical domain are converted into the computational domain and are shown in Figures 1 and 2 for the physical and computational domains, respectively. In these figures the Cartesian velocity components are located in the center of the cell and the contravariant velocity components are located at the

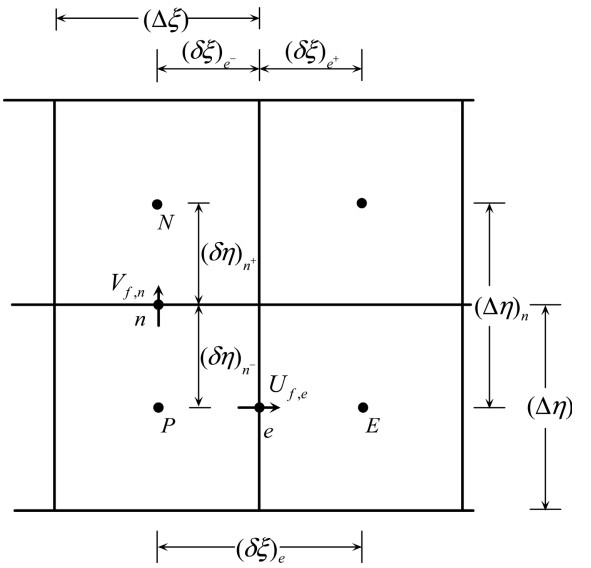

Figure 2. Geometry factor in the computational domain.

interfaces. The transferred governing equations are discretized in the computation domain with the finite-volume method (FVM) [13, 14]. The final discretized results are expressed as follows.

Continuity equation:

$$(\rho\,\Delta\eta\,U_f)_e - (\rho\,\Delta\eta\,U_f)_w + (\rho\,\Delta\xi\,V_f)_n - (\rho\,\Delta\xi\,V_f)_s = 0 \tag{11}$$

where U_f, V_f stand for the interface contravariant velocity components which are determined from the interpolated Cartesian velocity components at the interfaces.

Momentum equations:

$$\frac{A_P^u}{\alpha_u}u_P = \sum A_{\mathrm{nb}}^u u_{\mathrm{nb}} - B_P^u\frac{\partial p}{\partial\xi} - C_P^u\frac{\partial p}{\partial\eta} + b^u + \frac{1-\alpha_u}{\alpha_u}A_P^u u_P^0 \tag{12}$$

$$\frac{A_P^v}{\alpha_v}v_P = \sum A_{\mathrm{nb}}^v v_{\mathrm{nb}} - B_P^v\frac{\partial p}{\partial\xi} - C_P^v\frac{\partial p}{\partial\eta} + b^v + \frac{1-\alpha_v}{\alpha_v}A_P^v v_P^0 \tag{13}$$

In Eqs. (12) and (13), the underrelaxation factor is incorporated. The pressure gradient terms for u and v equations are calculated by

$$\frac{\partial p}{\partial\xi} = \frac{(p_e)_P - (p_w)_P}{\Delta\xi} \tag{14}$$

$$\frac{\partial p}{\partial\eta} = \frac{(p_n)_P - (p_s)_P}{\Delta\eta} \tag{15}$$

where the interface pressures $(p_e)_P$, $(p_w)_P$, $(p_n)_P$, $(p_s)_P$ are linearly interpolated from the values of the main nodes. The coefficients of Eqs. (12) and (13) are expressed as follows:

$$B_P^u = \left(\frac{\partial y}{\partial\eta}\right)_P\Delta\xi\,\Delta\eta \qquad C_P^u = -\left(\frac{\partial y}{\partial\xi}\right)_P\Delta\xi\,\Delta\eta \tag{16a}$$

$$B_P^v = -\left(\frac{\partial x}{\partial\eta}\right)_P\Delta\xi\,\Delta\eta \qquad C_P^v = \left(\frac{\partial x}{\partial\xi}\right)_P\Delta\xi\,\Delta\eta \tag{16b}$$

$$A_E = D_e A(|P_{\Delta e}|) + [[-F_e, 0]] \qquad A_W = D_w A(|P_{\Delta w}|) - [[F_w, 0]] \tag{17a}$$

$$A_N = D_n A(|P_{\Delta n}|) + [[-F_n, 0]] \qquad A_S = D_s A(|P_{\Delta s}|) - [[F_s, 0]] \tag{17b}$$

$$A_P = A_E + A_W + A_N + A_S \tag{18}$$

$$b^u = SJ\,\Delta\xi\,\Delta\eta - \left[\left(\frac{\Gamma}{J}\beta u_\eta\,\Delta\eta\right)\Big|_w^e + \left(\frac{\Gamma}{J}\beta u_\xi\,\Delta\xi\right)\Big|_s^n\right] \tag{19}$$

$$b^v = SJ\,\Delta\xi\,\Delta\eta - \left[\left(\frac{\Gamma}{J}\beta v_\eta\,\Delta\eta\right)\Big|_w^e + \left(\frac{\Gamma}{J}\beta v_\xi\,\Delta\xi\right)\Big|_s^n\right] \tag{20}$$

where F and D are flow rate and diffusion conductivity at the interface,

$$F_e = (\rho U\,\Delta\eta)_e \qquad F_w = (\rho U\,\Delta\eta)_w \tag{21a}$$

$$F_e = (\rho V\,\Delta\xi)_e \qquad F_w = (\rho V\,\Delta\xi)_w \tag{21b}$$

$$D_e = \left(\frac{\alpha}{J}\Gamma\,\frac{\Delta\eta}{\Delta\xi}\right)_e \qquad D_w = \left(\frac{\alpha}{J}\Gamma\,\frac{\Delta\eta}{\Delta\xi}\right)_w \tag{22a}$$

$$D_n = \left(\frac{\gamma}{J}\Gamma\,\frac{\Delta\xi}{\Delta\eta}\right)_n \qquad D_s = \left(\frac{\gamma}{J}\Gamma\,\frac{\Delta\xi}{\Delta\eta}\right)_s \tag{22b}$$

GENERAL REVIEW OF SIMPLE ALGORITHM

In the SIMPLE algorithm on a collocated nonorthogonal grid, the pressure in the source term of the momentum equations is obtained directly from the previous iteration. After solving the momentum equations, the interface Cartesian velocities are linearly interpolated from the values at the main nodes if the interpolation idea on the orthogonal grid system is applied, and the interface contravariant velocities are then determined based on the definition. The interface Cartesian velocities are determined by

$$u_e^* = \frac{(\delta\xi)_{e^-}}{(\delta\xi)_e}u_E^* + \frac{(\delta\xi)_{e^+}}{(\delta\xi)_e}u_P^* \qquad v_e^* = \frac{(\delta\xi)_{e^-}}{(\delta\xi)_e}v_E^* + \frac{(\delta\xi)_{e^+}}{(\delta\xi)_e}v_P^* \tag{23}$$

$$v_n^* = \frac{(\delta\eta)_{n^-}}{(\delta\eta)_n}v_N^* + \frac{(\delta\eta)_{n^+}}{(\delta\eta)_n}v_P^* \qquad u_n^* = \frac{(\delta\eta)_{n^-}}{(\delta\eta)_n}u_N^* + \frac{(\delta\eta)_{n^+}}{(\delta\eta)_n}u_P^* \tag{24}$$

The corresponding contravariant velocities are calculated as

$$\overline{U_e^*} = \left(u^*\frac{\partial y}{\partial\eta} - v^*\frac{\partial x}{\partial\eta}\right)_e = u_e^*(y_\eta)_e - v_e^*(x_\eta)_e \tag{25}$$

$$\overline{V_n^*} = \left(v^*\frac{\partial x}{\partial\xi} - u^*\frac{\partial y}{\partial\xi}\right)_n = v_n^*(x_\xi)_n - u_n^*(y_\xi)_n \tag{26}$$

It can be seen from Eqs. (25) and (26) that the so called $1-\delta$ pressure difference is not introduced and the including of which is the successful experience of staggered grids. Thus such an interpolation scheme may lead to an incorrect pressure distribution. To avoid an incorrect distribution, Rhie and Chow [15] proposed that an additional pressure gradient correction term be added to the right-hand side of Eqs. (25)

and (26). The final interface contravariant velocities are then expressed as

$$U_e^* = \overline{U_e^*} - B_{fe}^{0,u}\left(\frac{p_E - p_P}{\Delta\xi} - \bar{p}_\xi\right) \tag{27}$$

$$V_n^* = \overline{V_n^*} - C_{fn}^{0v}\left(\frac{p_N - p_P}{\Delta\eta} - \bar{p}_\eta\right) \tag{28}$$

where $\overline{U_e^*}$ and $\overline{V_n^*}$ are calculated by Eqs. (25) and (26), respectively.

Additional terms such as $[(p_N - p_P)/\Delta\eta] - \bar{p}_\eta$, are called smoothing terms, where $\bar{p}_\xi$ and $\bar{p}_\eta$ are the average pressure gradients in the ξ and η directions, respectively, for the control volume studied. Acharya and Moukalled [10] pointed that if Eqs. (27) and (28) are used to derive the pressure-correction equation, then the resulting equation is not the discretized continuity equation but rather is an approximate form of the continuity equation, and this will lead to mass nonconservative behavior despite the pressure oscillation being suppressed.

In the implementation of SIMPLER algorithm proposed by Acharya and Moukalled [10], the pressure is determined by the pressure equation in the prediction step, but no special attention is paid to the presence of the underrelaxation factor. In their SIMPLEM algorithm [10], the additional pressure correction term is avoided, yet the underrelaxation factor effect is not included. In addition, the Cartesian velocities are not updated in time while the interface contravariant velocities are improved.

As indicated in the introduction, the study of Choi [12] showed that the selection of contravariant velocities as cell face velocities may lead to unstable convergence, while the covariant selection reduces the satisfaction of the conservation law.

From the above brief discussion, it can be seen that (1) to incorporate the underrelaxation factor into the algorithm is of great importance to improve the robustness of the algorithm; and (2) to provide a good interpolation method is essential to avoid an additional correction term such that the conservation laws (both physical and geometric) can be satisfied.

In order to incorporate the above two ingredients into the algorithm for fluid flow and computation on a nonstaggered, nonorthogonal grid system, a new version of the SIMPLER algorithm, called SIMPLERM, is proposed. The details are presented in the following section.

MATHEMATICAL FORMULATION OF THE SIMPLERM ALGORITHM

In the SIMPELRM algorithm proposed in this study, the physical and geometric laws are satisfied by using the contravariant velocities as the cell face velocities and Cartesian components as the primary variables. A prediction step is added to solve the problems of selecting contravariant velocity components as cell face velocities when the grid is strongly nonorthogonal, as will be confirmed in the examples provided later. An appropriate interpolation method for interface contravariants is applied which can discard the additional pressure gradient correction term. Based on this practice, the checkerboard pressure distribution should be fully

avoided and the underrelaxation factor is combined into the iteration process on condition that the solution is underrelaxation factor independent.

The above descriptions are the main ideas of the SIMPLERM algorithm. It can be seen that the SIMPLERM algorithm is based on the SIMPLER algorithm but is an improved algorithm. The implementation of SIMPLERM algorithm is as follows.

Prediction Step of the SIMPLERM Algorithm

In one iteration of the SIMPLERM algorithm the pressure is first determined in the prediction step, which provides the source term for the momentum equation. In the derivation of the pressure equation, the underrelaxation factor is combined into the computational process.

Equations (12) and (13) are written in the explicit manner

$$u_P = \widehat{u_P^0} - B_{uP}^0 \left(\frac{\partial p}{\partial \xi}\right)_P - C_{uP}^0 \left(\frac{\partial p}{\partial \eta}\right)_P + (1-\alpha_u) u_p^0 \tag{29}$$

$$v_P = \widehat{v_P^0} - B_{vP}^0 \left(\frac{\partial p}{\partial \xi}\right)_P - C_{vP}^0 \left(\frac{\partial p}{\partial \eta}\right)_P + (1-\alpha_v) v_p^0 \tag{30}$$

where $\widehat{u_P^0}$ and $\widehat{v_P^0}$ are called pseudo-velocities:

$$\widehat{u_P^0} = \frac{\sum A_{\mathrm{nb}}^{0u} u_{\mathrm{nb}}^0 + b_P^{0u}}{(A_P^{0u})_P/\alpha_u} \qquad \widehat{v_P^0} = \frac{\sum A_{\mathrm{nb}}^{0v} v_{\mathrm{nb}}^0 + b_P^{0v}}{(A_P^{0v})_P/\alpha_v} \tag{31}$$

The b terms in Eq. (31) are calculated as follows:

$$b_P^{0u} = SJ\,\Delta\xi\,\Delta\eta - \left[\left(\frac{\Gamma}{J}\beta u_\eta^0\,\Delta\eta\right)\Big|_w^e + \left(\frac{\Gamma}{J}\beta u_\xi^0\,\Delta\xi\right)\Big|_s^n\right] \tag{32}$$

$$b_P^{0v} = SJ\,\Delta\xi\,\Delta\eta - \left[\left(\frac{\Gamma}{J}\beta v_\eta^0\,\Delta\eta\right)\Big|_w^e + \left(\frac{\Gamma}{J}\beta v_\xi^0\,\Delta\xi\right)\Big|_s^n\right] \tag{33}$$

The coefficients in Eqs. (29) and (30) are determined by

$$B_{uP}^0 = \frac{\alpha_u B_P^u}{(A_P^{0u})_P} = \frac{\alpha_u (y_\eta)_P\,\Delta\xi\,\Delta\eta}{(A_P^{0u})_P} \tag{34}$$

$$C_{uP}^0 = \frac{\alpha_u C_P^u}{(A_P^{0u})_P} = -\frac{\alpha_u (y_\xi)_P\,\Delta\xi\,\Delta\eta}{(A_P^{0u})_P} \tag{35}$$

$$B_{vP}^0 = \frac{\alpha_v B_P^v}{(A_P^{0v})_P} = -\frac{\alpha_v (x_\eta)_P\,\Delta\xi\,\Delta\eta}{(A_P^{0v})_P} \tag{36}$$

$$C_{vP}^0 = \frac{\alpha_v C_P^v}{(A_P^{0v})_P} = \frac{\alpha_v (x_\xi)_P \Delta\xi\,\Delta\eta}{(A_P^{0v})_P} \tag{37}$$

In the above equations, the superscript 0 means the values are obtained from the previous iteration. The interface Cartesian components are then gained by mimicking Eqs. (29) and (30):

$$u_e^0 = \widehat{u_e^0} - \left(B_u^0 \frac{\partial p}{\partial \xi}\right)_e - \left(C_u^0 \frac{\partial p}{\partial \eta}\right)_e + (1-\alpha_u) u_e^0 \tag{38}$$

$$v_e^0 = \widehat{v_e^0} - \left(B_v^0 \frac{\partial p}{\partial \xi}\right)_e - \left(C_v^0 \frac{\partial p}{\partial \eta}\right)_e + (1-\alpha_v) v_e^0 \tag{39}$$

$$u_n^0 = \widehat{u_n^0} - \left(B_u^0 \frac{\partial p}{\partial \xi}\right)_n - \left(C_u^0 \frac{\partial p}{\partial \eta}\right)_n + (1-\alpha_u) u_n^0 \tag{40}$$

$$v_n^0 = \widehat{v_n} - \left(B_v^0 \frac{\partial p}{\partial \xi}\right)_n - \left(C_v^0 \frac{\partial p}{\partial \eta}\right)_n + (1-\alpha_v) v_n^0 \tag{41}$$

Equations (38)–(41) can be regarded as the extension of the idea of the modified momentum interpolation method (MMIM) proposed by Majumdar [14] in orthogonal coordinates. In Eqs. (38)–(41), the coefficients are calculated as follows:

$$(B_u^0)_e = \frac{\alpha_u (y_\eta)_e (\delta\xi)_e \Delta\eta}{(A_P^{0u})_e} \qquad (C_u^0)_e = -\frac{\alpha_u (y_\xi)_e (\delta\xi)_e \Delta\eta}{(A_P^{0u})_e} \tag{42a}$$

$$(B_v^0)_e = -\frac{\alpha_v (x_\eta)_e (\delta\xi)_e \Delta\eta}{(A_P^{0v})_e} \qquad (C_v^0)_e = \frac{\alpha_v (x_\xi)_e (\delta\xi)_e \Delta\eta}{(A_P^{0v})_e} \tag{42b}$$

$$(B_u^0)_n = \frac{\alpha_u (y_\eta)_n \Delta\xi (\delta\eta)_n}{(A_P^{0u})_n} \qquad (C_u^0)_n = -\frac{\alpha_u (y_\xi)_n \Delta\xi (\delta\eta)_n}{(A_P^{0u})_n} \tag{42c}$$

$$(B_v^0)_n = -\frac{\alpha_v (x_\eta)_n \Delta\xi (\delta\eta)_n}{(A_P^{0v})_n} \qquad (C_v^0)_n = \frac{\alpha_v (x_\xi)_n \Delta\xi (\delta\eta)_n}{(A_P^{0v})_n} \tag{42d}$$

The variables at the interfaces $(\widehat{u_e^0}, \widehat{v_e^0}, \widehat{u_n^0}, \widehat{v_e^0})$ and the coefficients at the interfaces $[(A_P^u)_e, (A_P^v)_e, (A_P^u)_n, (A_P^v)_n]$ are linearly interpolated from the main points P, E, N:

$$(A_P^{0u})_e = \frac{(\delta\xi)_{e^-}}{(\delta\xi)_e}(A_P^{0u})_E + \frac{(\delta\xi)_{e^+}}{(\delta\xi)_e}(A_P^{0u})_P \quad (A_P^{0v})_e = \frac{(\delta\xi)_{e^-}}{(\delta\xi)_e}(A_P^{0v})_E + \frac{(\delta\xi)_{e^+}}{(\delta\xi)_e}(A_P^{0v})_P \tag{43a}$$

$$(A_P^{0u})_n = \frac{(\delta\eta)_{n^-}}{(\delta\eta)_n}(A_P^{0u})_N + \frac{(\delta\eta)_{n^+}}{(\delta\eta)_n}(A_P^{0u})_P \quad (A_P^{0v})_n = \frac{(\delta\eta)_{n^-}}{(\delta\eta)_n}(A_P^{0v})_N + \frac{(\delta\eta)_{n^+}}{(\delta\eta)_n}(A_P^{0v})_P \tag{43b}$$

$$\widehat{u_e^0} = \frac{(\delta\xi)_{e^-}}{(\delta\xi)_e}\widehat{u_E^0} + \frac{(\delta\xi)_{e^+}}{(\delta\xi)_e}\widehat{u_P^0} \quad \widehat{v_e^0} = \frac{(\delta\xi)_{e^-}}{(\delta\xi)_e}\widehat{v_E^0} + \frac{(\delta\xi)_{e^+}}{(\delta\xi)_e}\widehat{v_P^0} \tag{44a}$$

$$\widehat{u_n^0} = \frac{(\delta\eta)_{n^-}}{(\delta\eta)_n}\widehat{u_N^0} + \frac{(\delta\eta)_{n^+}}{(\delta\eta)_n}\widehat{u_P^0} \quad \widehat{v_n^0} = \frac{(\delta\eta)_{n^-}}{(\delta\eta)_n}\widehat{v_N^0} + \frac{(\delta\eta)_{n^+}}{(\delta\eta)_n}\widehat{v_P^0} \tag{44b}$$

The interface contravariant velocity components are defined as

$$U_e = \left(u\frac{\partial y}{\partial \eta} - v\frac{\partial x}{\partial \eta} \right)_e \tag{45}$$

$$V_n = \left(v\frac{\partial x}{\partial \xi} - u\frac{\partial y}{\partial \xi} \right)_n \tag{46}$$

Equations (38) and (39) are now substituted into Eq. (45), and Eqs. (40) and (41) are substituted into Eq. (46) to obtain interface contravariant velocity components:

$$U_e = \left(\widehat{u^0}\frac{\partial y}{\partial \eta} - \widehat{v^0}\frac{\partial x}{\partial \eta} \right)_e - \left(B_f^{0u}\frac{\partial p}{\partial \xi} \right)_e + \left(C_f^{0u}\frac{\partial p^0}{\partial \eta} \right)_e + (1-\alpha_u)(y_\eta)_e u_e^0 - (1-\alpha_v)(x_\eta)_e v_e^0 \tag{47}$$

$$V_n = \left(\widehat{v^0}\frac{\partial x}{\partial \xi} - \widehat{u^0}\frac{\partial y}{\partial \xi} \right)_n + \left(B_f^{0v}\frac{\partial p^0}{\partial \xi} \right)_n - \left(C_f^{0v}\frac{\partial p}{\partial \eta} \right)_n + (1-\alpha_v)(x_\xi)_n v_n^0 - (1-\alpha_u)(y_\xi)_n u_n^0 \tag{48}$$

where

$$B_{fe}^{0u} = B_{ue}^0 y_\eta - B_{ve}^0 x_\eta = \left(\frac{\alpha_u y_\eta^2}{A_P^{0u}} + \frac{\alpha_v x_\eta^2}{A_P^{0v}} \right)_e (\delta\xi)_e \Delta\eta \tag{49a}$$

$$C_{fe}^{0u} = -C_{ue}^0 y_\eta + C_{ve}^0 x_\eta = \left(\frac{\alpha_u y_\xi y_\eta}{A_P^{0u}} + \frac{\alpha_v x_\xi x_\eta}{A_P^{0v}} \right)_e (\delta\xi)_e \Delta\eta \tag{49b}$$

$$B_{fn}^{0v} = -B_{vn}^0 x_\xi + B_{un}^0 y_\xi = \left(\frac{\alpha_v y_\xi y_\eta}{A_P^{0u}} + \frac{\alpha_n x_\xi x_\eta}{A_P^{0v}} \right)_n (\delta\eta)_n \Delta\xi \tag{50a}$$

$$C_{fn}^{0v} = C_{vn}^0 x_\xi - C_{un}^0 y_\xi = \left(\frac{\alpha_v y_\xi^2}{A_P^{0u}} + \frac{\alpha_u x_\xi^2}{A_P^{0v}} \right)_n (\delta\eta)_n \Delta\xi \tag{50b}$$

It can be seen that in the interfacial contravariant components, Eqs. (47) and (48), the velocity underrelaxation factors are included. In order to guarantee that the solution is independent of the underrelaxation factor, the underrelaxation factors for the u momentum equation and the v momentum equation are set to be identical but not equal to 1, that is, $(\alpha = \alpha_u = \alpha_v \neq 1)$. Then Eqs. (47) and (48) can be rewritten as

$$U_e = \left(\widehat{u^0}\frac{\partial y}{\partial \eta} - \widehat{v^0}\frac{\partial x}{\partial \eta} \right)_e - \left(B_f^{0u}\frac{\partial p}{\partial \xi} \right)_e + \left(C_f^{0u}\frac{\partial p^0}{\partial \eta} \right)_e + (1-\alpha)\, U_e^0 \tag{51}$$

$$V_n = \left(\widehat{v^0}\frac{\partial x}{\partial \xi} - \widehat{u^0}\frac{\partial y}{\partial \xi} \right)_n + \left(B_f^{0v}\frac{\partial p^0}{\partial \xi} \right)_n - \left(C_f^{0v}\frac{\partial p}{\partial \eta} \right)_n + (1-\alpha)\, V_n^0 \tag{52}$$

The coefficients B_{fe}^{0u}, C_{fe}^{0u}, B_{fn}^{0v}, C_{fn}^{0v} are recast as

$$B_{fe}^{0u} = B_{ue}^{0} y_\eta - B_{ve}^{0} x_\eta = \left(\frac{y_\eta^2}{A_P^{0u}} + \frac{x_\eta^2}{A_P^{0v}} \right)_e \alpha(\delta\xi)_e \, \Delta\eta \tag{53a}$$

$$C_{fe}^{0u} = -C_{ue}^{0} y_\eta + C_{ve}^{0} x_\eta = \left(\frac{y_\xi y_\eta}{A_P^{0u}} + \frac{x_\xi x_\eta}{A_P^{0v}} \right)_e \alpha(\delta\xi)_e \, \Delta\eta \tag{53b}$$

$$B_{fn}^{0v} = -B_{vn}^{0} x_\xi + B_{un}^{0} y_\xi = \left(\frac{y_\xi y_\eta}{A_P^{0u}} + \frac{x_\xi x_\eta}{A_P^{0v}} \right)_n \alpha(\delta\eta)_n \, \Delta\xi \tag{54a}$$

$$C_{fn}^{0v} = C_{vn}^{0} x_\xi - C_{un}^{0} y_\xi = \left(\frac{y_\xi^2}{A_P^{0u}} + \frac{x_\xi^2}{A_P^{0v}} \right)_n \alpha(\delta\eta)_n \Delta\xi \tag{54b}$$

By introducing the pseudo-contravariant velocity components,

$$\widehat{U_e^0} = \left(\widehat{u^0} \frac{\partial y}{\partial \eta} - \widehat{v}^0 \frac{\partial x}{\partial \eta} \right)_e + \left(C_f^{0u} \frac{\partial p}{\partial \eta} \right)_e + (1-\alpha) U_e^0 \tag{55}$$

$$\widehat{V_n^0} = \left(\widehat{v^0} \frac{\partial x}{\partial \xi} - \widehat{u^0} \frac{\partial y}{\partial \xi} \right)_n + \left(B_f^{0v} \frac{\partial p}{\partial \xi} \right)_n + (1-\alpha) V_n^0 \tag{56}$$

Eqs. (51) and (52) can be rewritten as

$$U_e = \widehat{U_e^0} - \left(B_f^{0u} \frac{\partial p}{\partial \xi} \right)_e \tag{57}$$

$$V_n = \widehat{V_n^0} - \left(C_f^{0v} \frac{\partial p}{\partial \eta} \right)_n \tag{58}$$

By substituting Eqs. (57) and (58) into the continuity equation, Eq. (11), we get the pressure equation:

$$A_P^0 p_P^* = \sum A_{\mathrm{nb}}^0 p_{\mathrm{nb}}^* + b \tag{59}$$

where

$$A_P^0 = A_E^0 + A_W^0 + A_N^0 + A_S^0 \tag{60}$$

$$(A_E^0)_P = (A_W^0)_E = \left(\frac{\rho \, \Delta\eta \, B_f^{0u}}{\delta\xi} \right)_e \tag{61}$$

$$(A_N^0)_P = (A_S^0)_N = \left(\frac{\rho \, \Delta\xi \, C_f^{0v}}{\delta\eta} \right)_n \tag{62}$$

$$b = (\rho \Delta\eta \, \widehat{U^0}) \Big|_e^w + (\rho \, \Delta\xi \, \widehat{V^0}) \Big|_n^s \tag{63}$$

To further improve the robustness of the algorithm, the pressure underrelaxation factor α_p is also incorporated. The final form of the pressure equation in the prediction step can be expressed as

$$\frac{A_P^0}{\alpha_p} p_P^* = \sum A_{\mathrm{nb}}^0 p_{\mathrm{nb}}^* + b + \frac{1-\alpha_p}{\alpha_p} A_P^0 p_P^0 \tag{64}$$

The pressure solved from the pressure equation is used to calculate the source term of the momentum equation. The discretized momentum equations are then solved to update the Cartesian velocities at the main node, and the resulting velocities are defined by u^*, v^*. Then the interface contravariant velocities components are determined directly, based on the updated Cartesian velocities at the main nodes.

The intermediate interface contravariant velocity components are determined by a modified momentum interpolation method based on Eqs. (38)–(41), in which the underrelaxation factor is incorporated under the condition of $\alpha_u = \alpha_v = \alpha \neq 1$. The modified interpolation details are as follows.

On the condition of $\alpha_u = \alpha_v = \alpha \neq 1$, Eq. (31) is recast as

$$\widehat{u_P^i} = \frac{\sum A_{\mathrm{nb}}^{0u} u_{\mathrm{nb}}^* + b_P^{0u}}{(A_P^{0u})_P/\alpha} \qquad \widehat{v_P^i} = \frac{\sum A_{\mathrm{nb}}^{0v} v_{\mathrm{nb}}^* + b_P^{0v}}{(A_P^{0v})_P/\alpha} \tag{65}$$

In Eq. (65), the $\widehat{u_P^i}$, $\widehat{v_P^i}$ terms represent the intermediate grid pseudo-Cartesian velocities. The corresponding interface pseudo-Cartesian velocities are linearly interpolated as

$$\widehat{u_e^i} = \frac{(\delta\xi)_{e^-}}{(\delta\xi)_e}\widehat{u_E^i} + \frac{(\delta\xi)_{e^+}}{(\delta\xi)_e}\widehat{u_P^i} \qquad \widehat{v_e^i} = \frac{(\delta\xi)_{e^-}}{(\delta\xi)_e}\widehat{v_E^i} + \frac{(\delta\xi)_{e^+}}{(\delta\xi)_e}\widehat{v_P^i} \tag{66}$$

$$\widehat{u_n^i} = \frac{(\delta\eta)_{n^-}}{(\delta\eta)_n}\widehat{u_N^i} + \frac{(\delta\eta)_{n^+}}{(\delta\eta)_n}\widehat{u_P^i} \qquad \widehat{v_n^i} = \frac{(\delta\eta)_{n^-}}{(\delta\eta)_n}\widehat{v_N^i} + \frac{(\delta\eta)_{n^+}}{(\delta\eta)_n}\widehat{v_P^i} \tag{67}$$

Similar to the deviation of Eqs. (51) and (52), the intermediate interface contravariant velocity components are obtained with the modified momentum interpolation:

$$U_e^* = \left(\widehat{u^i}\frac{\partial y}{\partial\eta} - \widehat{v^i}\frac{\partial x}{\partial\eta}\right)_e - \left(B_f^{0u}\frac{\partial p^*}{\partial\xi}\right)_e + \left(C_f^{0u}\frac{\partial p^*}{\partial\eta}\right)_e + (1-\alpha)U_e^0 \tag{68}$$

$$V_n^* = \left(\widehat{v^i}\frac{\partial x}{\partial\xi} - \widehat{u^i}\frac{\partial y}{\partial\xi}\right)_n + \left(B_f^{0v}\frac{\partial p^*}{\partial\xi}\right)_n - \left(C_f^{0v}\frac{\partial p^*}{\partial\eta}\right)_n + (1-\alpha)V_n^0 \tag{69}$$

The coefficients B_f^{0u}, C_f^{0u}, B_f^{0v}, and C_f^{0v} are calculated by Eqs. (53) and (54). It should be emphasized that Eqs. (68) and (69) are consistent with Eqs. (51) and (52); the only difference is the computational levels. Equations (51) and (52) are based on the previous velocities u^0, v^0, while Eqs. (68) and (69) are based on the intermediate velocities u^i, v^i. It is clear that the $1-\delta$ pressure difference is introduced to prevent oscillation of the pressure field. When iteration converges, U_e^* and V_n^* are equal to

U_e^0 and V_n^0, respectively, and the effect of the underrelaxation factor is eliminated, making the final solution independent of the underrelaxation factor.

The use of Eqs. (68) and (69) can fully discard the additional pressure gradient term in Eqs. (27) and (28), so the SIMPLERM algorithm can guarantee the mass conservation of control volumes. This is the key difference between the SIMPLE and SIMPLERM algorithms.

Correction Step of the SIMPLERM Algorithm

The interface velocities U_e^*, V_n^*, which do not satisfy the continuity equation need to be improved to satisfy the continuity equation. Based on Eqs. (29) and (30), the velocity correction at the main node is obtained after neglecting the neighboring velocity correction. The velocity corrections for u and v are then expressed as

$$u'_P = -B^0_{uP}\frac{\partial p'}{\partial \xi} - C^0_{uP}\frac{\partial p'}{\partial \eta} \tag{70}$$

$$v'_P = -B^0_{vP}\frac{\partial p'}{\partial \xi} - C^0_{vP}\frac{\partial p'}{\partial \eta} \tag{71}$$

The improved velocities at the main node are expressed as

$$u_P = u^*_p + u'_P \tag{72}$$

$$v_P = v^*_p + v'_P \tag{73}$$

The intermediate contravariant velocities at the main node are

$$U_P = \left(u^*\frac{\partial y}{\partial \eta} - v^*\frac{\partial x}{\partial \eta}\right)_P \tag{74}$$

$$V_P = \left(v^*\frac{\partial x}{\partial \xi} - u^*\frac{\partial y}{\partial \xi}\right)_P \tag{75}$$

The corresponding contravariant velocity corrections at the main node are

$$U'_P = \left(u'\frac{\partial y}{\partial \eta} - v'\frac{\partial x}{\partial \eta}\right)_P \tag{76}$$

$$V'_P = \left(v'\frac{\partial x}{\partial \xi} - u'\frac{\partial y}{\partial \xi}\right)_P \tag{77}$$

Equations (70) and (71) are substituted into Eqs. (76) and (77):

$$U'_P = (-y_\eta B^0_{uP} + x_\eta B^0_{vP})p'_\xi + (-y_\eta C^0_{uP} + x_\eta C^0_{vP})p'_\eta \tag{78}$$

$$V'_P = (-x_\xi C^0_{vP} + y_\xi C^0_{uP})p'_\eta + (-x_\xi B^0_{vP} + y_\xi B^0_{uP})p'_\xi \tag{79}$$

To obtain the pressure-correction equation of a five-point computational molecule, the p'_η in Eq. (78) and the p'_ξ term in Eq. (79) are omitted, so the final contravariant velocity corrections at the main node are expressed as

$$U'_P = (-y_\eta B^0_{uP} + x_\eta B^0_{vP}) p'_\xi \tag{80}$$

$$V'_P = (-x_\xi C^0_{vP} + y_\xi C^0_{uP}) p'_\eta \tag{81}$$

By mimicking Eqs. (80) and (81), the interface contravariant velocity components are obtained as

$$U'_e = -B^{0u}_{fe} p'_\xi \tag{82}$$

$$V'_n = -C^{0v}_{fn} p'_\eta \tag{83}$$

where the coefficients of B^{0u}_{fe} and C^{0v}_{fn} are calculated by Eqs. (53*a*) and (54*b*). With the pressure-correction term, the improved interface contravariant velocities can be expressed as

$$U_e = U^*_e - \left(B^{0u}_f \frac{\partial p'}{\partial \xi} \right)_e \tag{84}$$

$$V_n = V^*_n - \left(C^{0v}_f \frac{\partial p'}{\partial \eta} \right)_n \tag{85}$$

Equations (84) and (85) are substituted into the continuity equation, and the pressure-correction equation in the correction step is thus obtained.

$$A^0_P p'_p = \sum A^0_{\mathrm{nb}} p'_{\mathrm{nb}} + b \tag{86}$$

The coefficients A_P, A_E, A_W, A_N, and A_S are determined by Eqs. (60)–(62), and the term b is calculated based on the intermediate interface contravariant velocity,

$$b = (\rho \, \Delta\eta \, U^*_f)\big|^w_e + (\rho \, \Delta\xi \, V^*_f)\big|^s_n \tag{87}$$

CALCULATION PROCEDURE FOR SIMPLERM ALGORITHM

The calculation procedure for the SIMPLERM algorithm can be expressed as follows.

1. Assume the initial velocity field u^0_P, v^0_P, U^0_f, V^0_f.
2. Based on the interface contravariant velocity and the Cartesian velocity at the main nodes, calculate the coefficient of the momentum equation and interface pseudo-contravariant velocities $\widehat{U^0_e}$ by Eq. (55) and $\widehat{V^0_n}$ by Eq. (56).
3. Calculate the related coefficients of the pressure equation, B^{0u}_{fe} by Eq. (53*a*) and C^{0v}_{fn} by Eq. (54*b*).
4. Solve the pressure equation (64) and obtain the pressure field p^*.

5. Calculate the source term of the momentum equation by Eqs. (14) and (15) on p^* and solve the momentum equations to obtain the intermediate velocities u_P^* and v_P^*.
6. Calculate the intermediate contravariant velocities, U_e^* by Eq. (68) and V_n^* by Eq. (69).
7. Solve the pressure-correction equation, Eq. (86), to obtain the pressure-correction term p'.
8. Obtain the improved interface contravariant velocities, U_e by Eq. (84) and V_n by Eq. (85), and the Cartesian velocities at the main node, u_P by Eq. (72) and v_P by Eq. (73).
9. Calculate the coefficients of other general variable if coupled with velocities and solve the discretized equations.
10. Return to step 2 and repeat until convergence is reached.

To sum up, in the proposed algorithm the contravariant velocity components are taken as the cell face velocities, and this guarantees satisfaction of the conservation laws. The $1 - \delta$ pressure difference introduced in steps (6) and (7) can effectively prevent pressure field oscillation. The underrelaxation factor is combined into the calculation procedure, which improves robustness while not affecting the final converged solution. Finally, the additional pressure-correction term is avoided, and the mass conservation law can be satisfied with sufficient accuracy.

TEST PROBLEMS AND RESULTS

In order to test the feasibility of the proposed SIMPLERM algorithm when the grid is strongly nonorthogonal, the flow in a cavity with a moving lid and inclined side walls proposed by Demirdzic and Peric [17] is solved. Two typical inclinations with $\beta = 30^\circ$ and 45° are tested separately for comparison. Peric [18] pointed out that if the nonorthogonal term is omitted in the derivation of the pressure-correction equation, the algorithm became inefficient when the angles between grid lines approach 45°, and it usually fails to converge when the angles fall below 30°. So in the calculation for these two typical cases in [17], the cross-derivatives resulting from nonorthogonality are treated implicitly, leading to the pressure correction being a nine-point computational molecule for 2-D problem. In the SIMPLERM algorithm of this study, the nonorthogonal term is also dropped to gain a five-point pressure-correction equation. By using an appropriate prediction step and underrelaxation factor, the SIMPLERM algorithm shows good performance for these two typical cases.

The geometry and boundary condition are displayed in Figure 3. The governing equations are omitted for simplification of presentation. Computation is conducted with $\mathrm{Re} = 1{,}000$, and the adopted mesh is 103×103. The Reynolds number is defined as

$$\mathrm{Re} = \frac{\rho \cdot u_L \cdot L}{\eta} \tag{88}$$

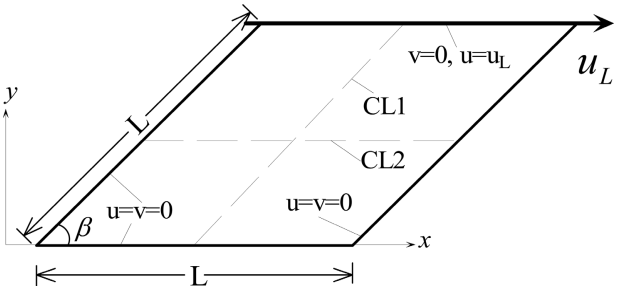

Figure 3. Computation domain and boundary conditions.

The meshes are generated with the Poisson equation [16], and are represented in Figure 4 for $\beta = 45^\circ$ and 30°. To demonstrate the effectiveness of SIMPLERM to overcome the shortcoming of nonsatisfaction of local mass conservation, four mass and momentum residuals are defined. The first is the maximum mass residue of control volumes, called $RS_{max\,1}$, in which the interface contravariant velocity does not include the smoothing term. The second residual is the maximum mass residue of control volumes, called $RS_{max\,2}$, in which the interface contravariant velocity is added by the smoothing term. The last two residuals are the maximum momentum equation residuals for u and v, called RS_u and RS_v, respectively. The expressions of the above four residuals are

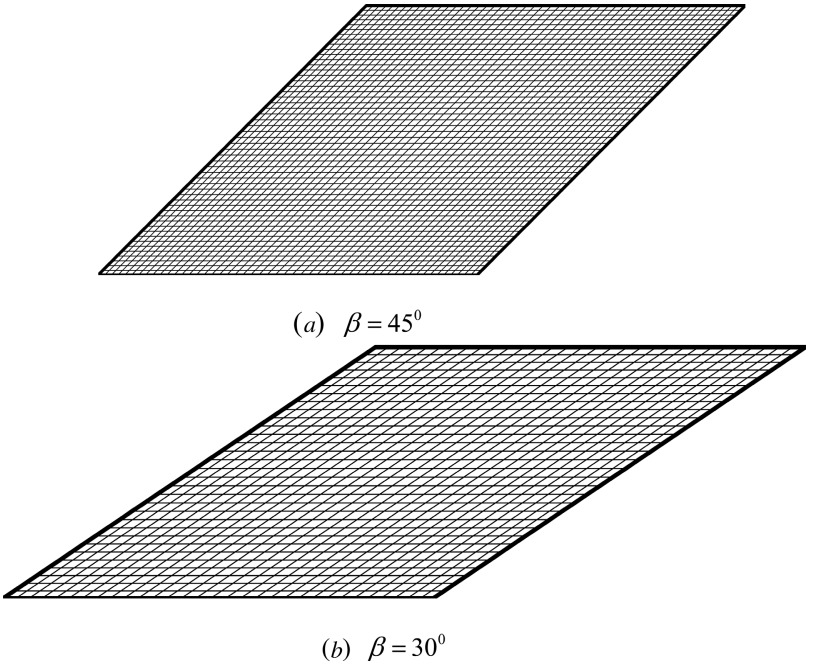

Figure 4. Generated grid distribution.

$$\mathrm{RS}_{\max 1} = \left[(\rho \Delta\eta \, \overline{U_f^*})\big|_e^w + (\rho \Delta\xi \, \overline{V_f^*})\big|_n^s \right]_{\max} \tag{89}$$

$$\mathrm{RS}_{\max 2} = \left[(\rho \Delta\eta \, U_f^*)\big|_e^w + (\rho \Delta\xi \, V_f^*)\big|_n^s \right]_{\max} \tag{90}$$

$$R_{su} = \left\{ \sum_{NEWS} \left[\frac{A_P^{*u}}{\alpha_u} u_P - \left(\sum A_{\mathrm{nb}}^{*u} u_{\mathrm{nb}} - B_P^u \frac{\partial p^*}{\partial \xi} - C_P^u \frac{\partial p^*}{\partial \eta} + b^u + \frac{1-\alpha_u}{\alpha_u} A_P^{*u} u_P^* \right) \right]^2 \right\}_{\max}^{1/2} \tag{91}$$

$$R_{sv} = \left\{ \sum_{NEWS} \left[\frac{A_P^{*v}}{\alpha_v} v_P - \left(\sum A_{\mathrm{nb}}^{*v} v_{\mathrm{nb}} - B_P^v \frac{\partial p^*}{\partial \xi} - C_P^v \frac{\partial p^*}{\partial \eta} + b^v + \frac{1-\alpha_u}{\alpha_u} A_P^{*u} v_P^* \right) \right]^2 \right\}_{\max}^{1/2} \tag{92}$$

In Eqs. (89) and (90), $\overline{U_f^*}$ and $\overline{V_f^*}$ are calculated from Eqs. (25) and (26), respectively, and U_f^* and V_f^* are obtained with Eqs. (27) and (28), respectively, which occur in the source terms of the pressure equations. Figures 5 and 6 show the convergence histories for the solution procedures using SIMPLE and SIMPLERM, respectively. In Figure 5, the two maximum mass residuals and two momentum equation residuals obtained by using SIMPLE algorithm for $\beta = 45°$ and $30°$ are presented. It can be found that the two residuals of the momentum equations and $\mathrm{RS}_{\max 2}$ are driven to zero with iteration; however, the real residue of continuity equation $\mathrm{RS}_{\max 1}$ remains at a certain level of about 4×10^{-4}. The predicted tendency shown in Figure 5 indicates that the integral form of the continuity equation is not actually satisfied because of the existence of the correction term added to the interface contravariant velocities. As a result, the interface contravariant velocities are no longer exactly equal to the real ones in the local mass conservation, which leads to the result

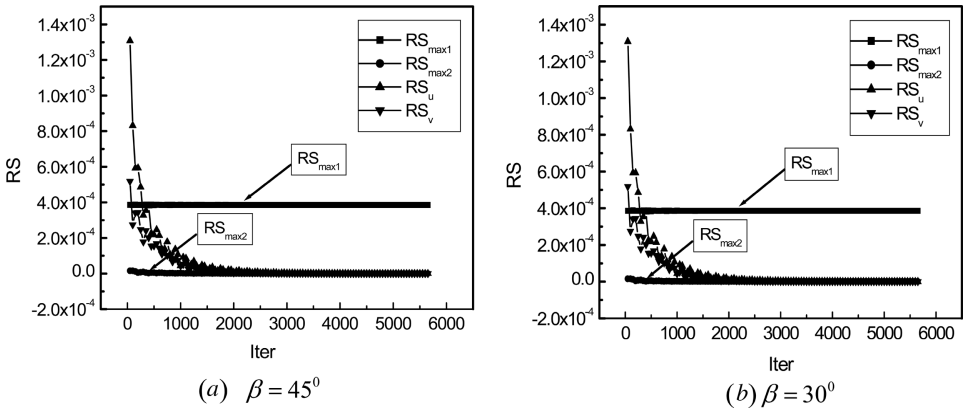

(a) $\beta = 45^0$ (b) $\beta = 30^0$

Figure 5. Residuals variation of SIMPLE algorithm with different inclined walls.

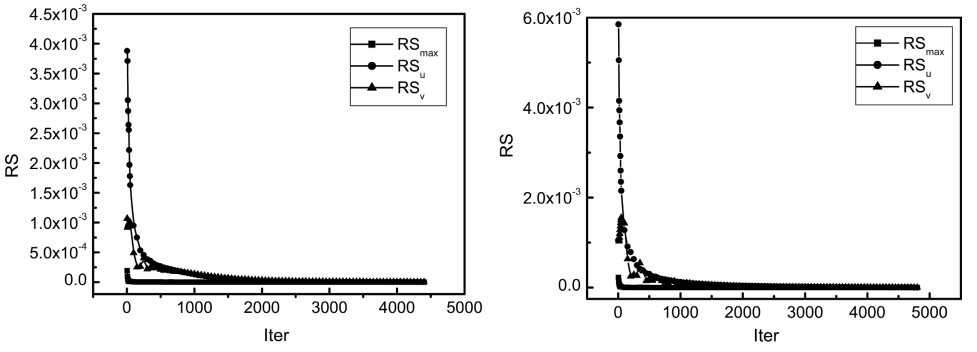

(a) $\beta = 45^0$ (b) $\beta = 30^0$

Figure 6. Residuals variation of SIMPLERM algorithm with different inclined walls.

that the solved pressure-correction equation is not the discretized continuity equation but rather an approximate form.

For the SIMPLERM algorithm, the mass residue $\mathrm{RS}_{\max}$ is defined as

$$\mathrm{RS}_{\max} = (\rho \Delta\eta \, U_f^*)\big|_e^w + (\rho \Delta\xi \, V_f^*)\big|_n^s \tag{93}$$

In Eq. (93), U_f^* and V_f^* are calculated by Eqs. (68) and (69), in which no additional term is introduced. The variation tendency of the residues $\mathrm{RS}_{\max 2}$, RS_u, and RS_v are displayed in Figure 6 for the two inclined wall angles. It is shown that all the residues decrease to zero with iteration, which implies that satisfaction of the continuity equation is fully realized.

It is specially noted that when the grid nonorthogonality is significant (the wall inclined angle is 30°), the unsteady convergence histories described in [12] do not occurs in the present study.

The stream function results of the SIMPLERM algorithm and [17] are presented in Figures 7 and 8 for two inclined cases. It can be seen that the two results are in good agreement. The numerical results further confirm the prediction accuracy of SIMPLERM.

In order to evaluate the robustness of the SIMPLERM algorithm in a wide range, the time-step multiple, E, instead of the underrelaxation factor, is used, which is related to the underrelaxation factor α by Eq. (94) [19]:

$$E = \frac{\alpha}{1-\alpha} \qquad (0 < \alpha < 1) \tag{94}$$

Some correspondence between α and E is presented in Table 2. The calculation is conducted with the SIMPLERM algorithm for $\mathrm{Re} = 1{,}000$. The convergence criterion is that the nondimensional mass residual $\mathrm{RS}_{\max}$ is less than 5.0×10^{-8}. Figure 9 shows the relation of iteration number and E. It can be seen that a converged solution can be reached for underrelaxation factor varying from 0.1 to 0.5.

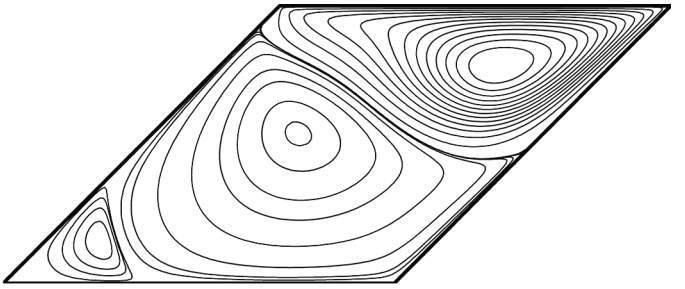

(*a*) Results of SIMPLERM

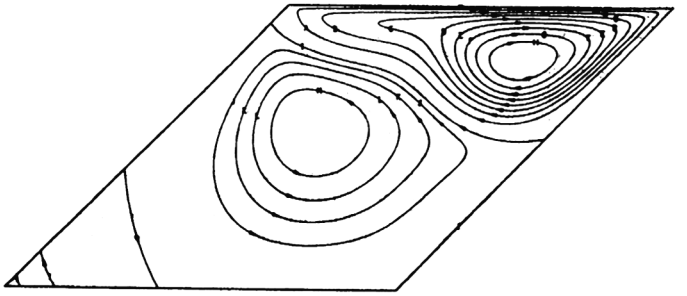

(*b*) Results of reference [17]

Figure 7. Stream function comparison with $\beta = 45^{\circ}$.

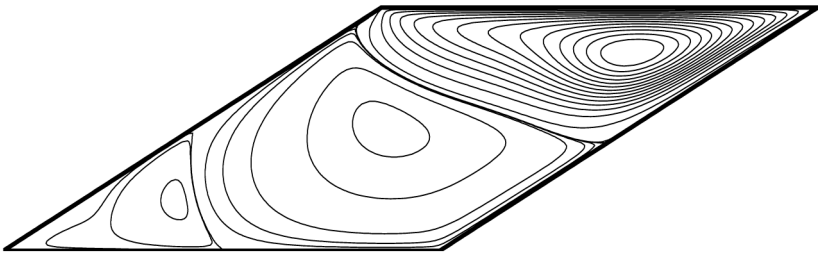

(*a*) Results of SIMPLERM

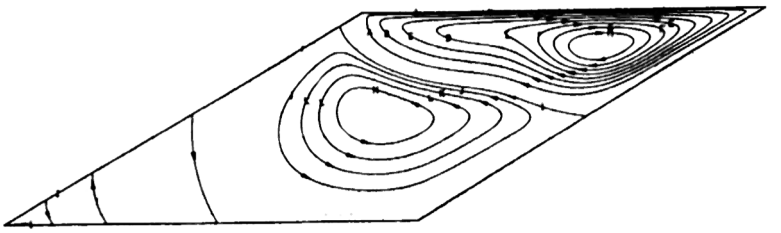

(*b*) Results of reference [17]

Figure 8. Stream function comparison with $\beta = 30^{\circ}$.

Table 2. Some correspondence between α and E

α	0.1	0.2	0.3	0.4	0.5	0.6	0.7	0.8	0.9	0.95
E	0.111	0.25	0.428	0.66	1	1.5	2.33	4	9	19

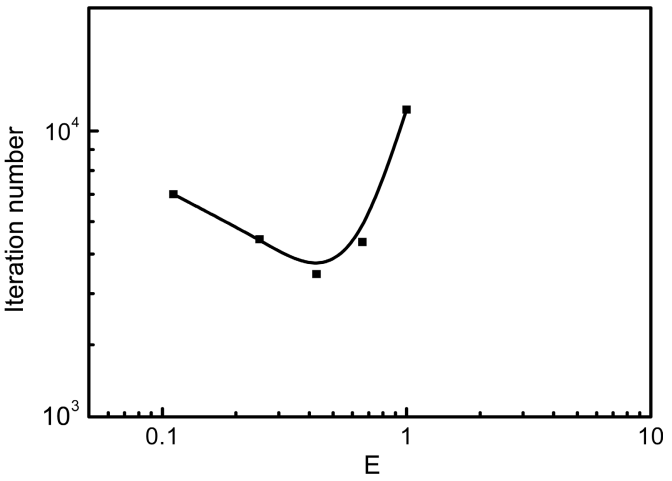

(*a*) $\beta = 45^0$

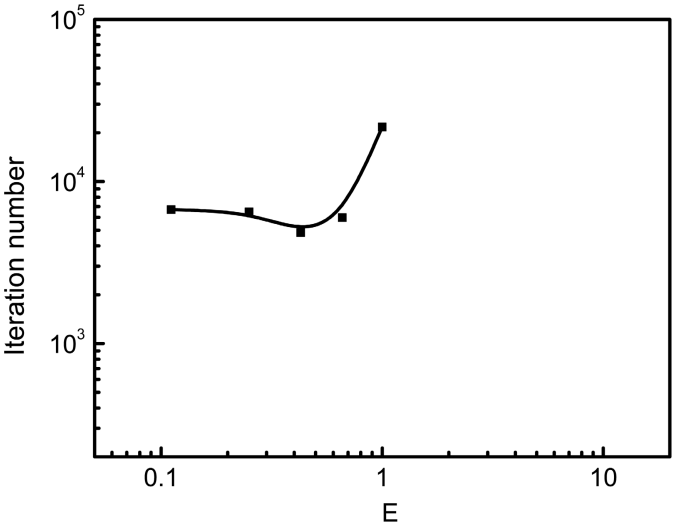

(*b*) $\beta = 30^0$

Figure 9. Variation of iteration number with E.

The robustness can be seen to be quite good with the pressure-correction equation of a five-point computational molecule.

To examine the capability of the SIMPLERM algorithm for the coupling between velocity and pressure, the predicted pressure profiles along section CL2 are shown in Figure 10 for $\beta = 45^\circ$ and 30° for the underrelaxation factor 0.1. The reference pressure point is the center of the left side wall. It can be obviously observed that no zigzag pressure field is predicted. This result shows that the SIMPLEM algorithm can damp out the false pressure field successfully.

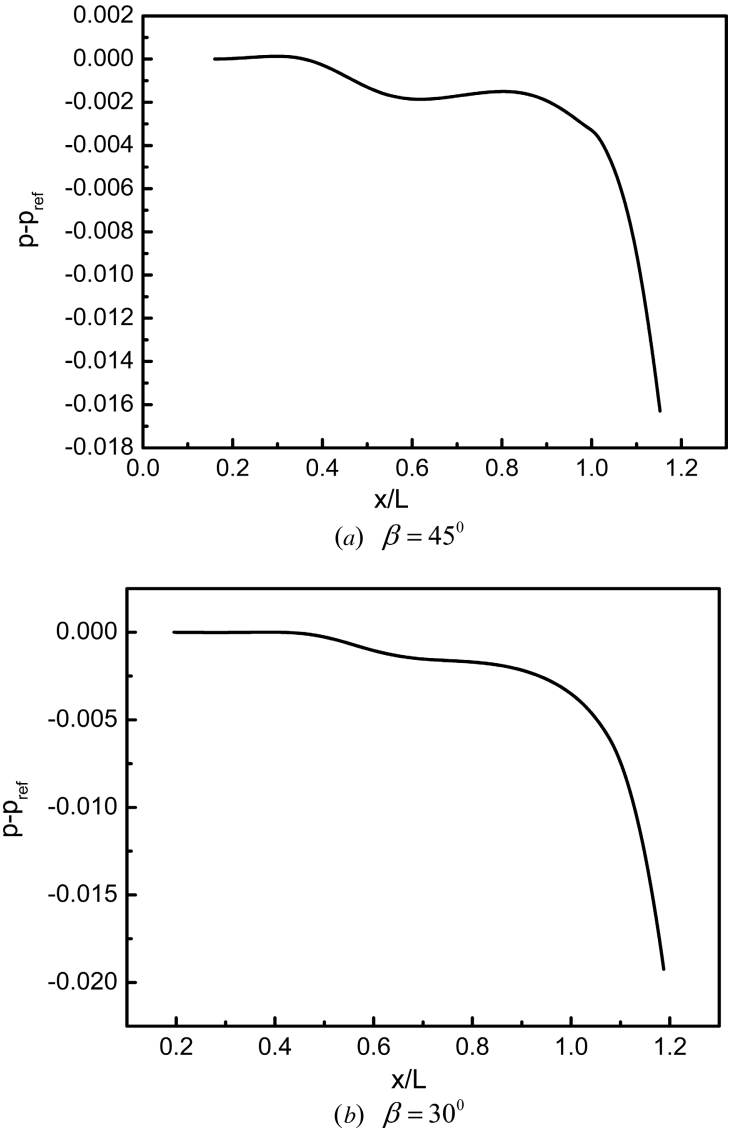

Figure 10. Pressure profile along section CL2.

Table 3. Velocity values with different underrelaxation factors ($\beta = 45°$)

	α				
Variable	0.1	0.2	0.3	0.4	0.5
u	0.25780	0.25785	0.25782	0.25789	0.25792
v	6.1104E-2	6.1114E-2	6.1108E-2	6.1105E-2	6.1100E-2

Table 4. Velocity values with different underrelaxation factors ($\beta = 30°$)

	α				
Variable	0.1	0.2	0.3	0.4	0.5
u	0.25488	0.25476	0.25480	0.25435	0.25496
v	3.5618E-2	3.5642E-2	3.5675E-2	3.5669E-2	3.5684E-2

To investigate the effect of the underrelaxation factor on the converged solution, typical values of velocities u and v in locations in section CL1 with y coordinate $0.45\sqrt{2}L$ under various underrelaxation factors are shown in Tables 3 and 4 for the two angles, respectively. It is obvious that the converged velocity solution is independent of the underrelaxation factor.

CONCLUSIONS

In this article, a modified algorithm named SIMPLERM is proposed to predict incompressible fluid flow and heat transfer on nonstaggered collocated grids. In the SIMPLERM algorithm, the contravariant velocity is chosen as cellface velocity and the underrelaxation factor is fully combined into the momentum interpolation on condition that the underrelaxation factors for u momentum and v momentum are identical but not equal to 1. The robustness of the algorithm is greatly improved. In the calculation of interface contravariant velocity, the SIMPLERM algorithm completely avoids the additional correction term and the prediction step is introduced to improve the convergence stability and robustness of the algorithm. Two typical numerical examples in nonorthogonal curvilinear coordinates are studied to confirm the feasibility of the SIMPLEM algorithm in terms of prediction accuracy, robustness, and stability.

REFERENCES

1. C. M. Rhie, A Numerical Study of the Flow Past an Isolated Airfoil with Separations, PhD thesis, University of Illinois, Urbana-Champaign, 1981.
2. M. Peric, A Finite Volume Method for the Predictions of Three-Dimensional Fluid Flow in Complex Ducts, PhD thesis, University of London, London, UK, 1985.
3. S. Majumdar, Development of a Finite-Volume Procedure for Prediction Fluid Flow Problems with Complex Irregular Boundaries, Rep. 210/T/29, SFB210, University of Karlsrule, Karlsrule, Germany, 1986.

4. S. Majumdar, Roles of Under-relaxation in Momentum Interpolation for Calculation of Flow with Non-staggered Grids, *Numer. Heat Transfer*, vol. 13, pp. 125–132, 1988.
5. T. F. Miller and F. W. Schmidt, Use of a Pressure-Weighted Interpolation Method for the Solution of Incompressible Navier-Stokes Equations on a Non-staggered Grid System, *Numer. Heat Transfer*, vol. 14, pp. 213–233, 1988.
6. S. K. Choi, Note on the Use of Momentum Interpolation Method for Unsteady Flows, *Numer. Heat Transfer A*, vol. 36, pp. 545–550, 1999.
7. M. H. Kobayashi and J. C. F. Pereira, Numerical Comparison of Momentum Interpolation Methods and Pressure-Velocity Algorithm Using Nonstaggered Grids, *Commun. Appl. Numer. Meth.*, vol. 7, pp. 173–196, 1991.
8. Z. G. Qu, W. Q. Tao, and Y. L. He, Implementation of CLEAR Algorithm on Collocated Grid System and Application Examples, *Numer. Heat Transfer B*, vol. 47, pp. 64–96, 2005.
9. W. Shyy and T. C. Vu, On the Adoption of Velocity Variable Grid System for Fluid Flow Computation in Curvilinear Coordinates, *J. Comput. Phys.*, vol. 92, pp. 82–105, 1991.
10. S. Acharya and F. H. Moukalled, Improvements to Incompressible Fluid Flow Calculation on a Non-staggered Curvilinear Grid, *Numer. Heat Transfer B*, vol. 15, pp. 131–152, 1989.
11. M. H. Kobayashi and J. C. F. Pereira, Calculation of Incompressible Laminar Flows on a Nonstaggered, Nonorthgonal Grid, *Numer. Heat Transfer B*, vol. 19, pp. 343–362, 1991.
12. S. K. Choi, H. Y. Nam, and M. Cho, Use of the Momentum Interpolation Method for Numerical Solution of Incompressible Flows in Complex Geometries: Choosing Cell Face Velocities, *Numer. Heat Transfer B*, vol. 23, pp. 21–41, 1993.
13. S. V. Patankar, *Numerical Heat Transfer and Fluid Flow*, Hemisphere, Washington, DC, 1980.
14. W. Q. Tao, *Recent Advances in Computational Heat Transfer*, pp. 192–196, Science Press, Beijing, 2000.
15. C. M. Rhie and W. L. Chow, Numerical Study of the Turbulent Flow past an Airfoil with Trading Edge Separations, *AIAA J.*, vol. 21, no. 11, pp. 1525–1535, 1983.
16. J. F. Thompson, Z. U. A. Warsi, and C. W. Mast, *Numerical Grid Generation, Foundation and Application*, North-Holland, New York, 1985.
17. I. Demirdzic and M. Peric, Finite Volume Method for Prediction of Fluid Flow in Arbitrarily Shaped Domains with Moving Boundaries, *Int. J. Numer. Meth. Fluids*, vol. 10, pp. 771–790, 1990.
18. M. Peric, Analysis of Pressure–Velocity Coupling on Nonorthgonal Grids, *Numer. Heat Transfer B*, vol. 17, pp. 63–82, 1999.
19. J. P. van Doormaal and G. D. Raithby, Enhancement of the SIMPLE Method for Predicting Incompressible Fluid Flow, *Numer Heat Transfer*, vol. 7, pp.147–163, 1984.